TENSILE CAPACITY OF STEEL PLATE CONNECTIONS WITH DIFFERENT BOLT DISTRIBUTION DUE TO TENSILE LOAD

AHMED M. SAYED

Department of Civil Engineering, College of Engineering, Assiut University, Assiut 71511, Egypt
Department of Civil and Environmental Engineering, College of Engineering, Majmaah
University, Al-Majmaah 11952, Saudi Arabia
E-mail: ahmed_m_sg@aun.edu.eg

Abstract

The use of bolted connections in the steel plate is an essential element in steel constructions as they are directly affecting the design of the steel sections, especially under the influence of tensile load. There are two types of bolts distribution in the connections: linear or staggered distribution, which depends on the number of bolts and the width of the steel section. The presence of the holes has an impact on the mechanical response of the steel structure. The objective of this paper is an experimental studying of the behaviour of net section tension capacity of steel plates with different types of bolted distribution under the axial tension force. To achieve this, the experimental tests were carried out on nine specimens to be used to investigate the effect of this condition and test the accuracy of current design codes. Experimental testing shows that the critical net section area is not always the smallest width but depends on the shape of the bolt's distribution, and the staggered distribution is often the critical section even if it is the longest in terms of net width. The efficiency of the shape of the bolts in a linear distribution affected the increase in the stress capacity of the steel plates, but in staggered bolts distribution, the stress reduction rate in the yielding and maximum ultimate stresses phase equals to 9.43% and 17.33% respectively. It can be concluded that the current design codes such as AISC and Eurocode-3 calculations of the ultimate stress capacities of linear bolts distribution are applicable and have some factor of safety. Nevertheless, on the other side, the codes calculations of the ultimate stress capacities of staggered bolts distribution are unsuitable for our case study and need a reduction coefficient at least equal to 0.744 just to get the actual stress of steel plate.

Keywords: Linear bolts distribution, Net section, Staggered distribution, Steel plates.

1. Introduction

Steel structures are the type of buildings that are exclusively built by steel connections. There are several ways to connect steel elements either by using bolts or by welding. Each of them has advantages and also disadvantages in the construction. When using bolted connections, holes are made in the steel plates to be connected, so some rules must be taken into account when making these holes according to the current design codes [1, 2] as shown in Fig. 1.
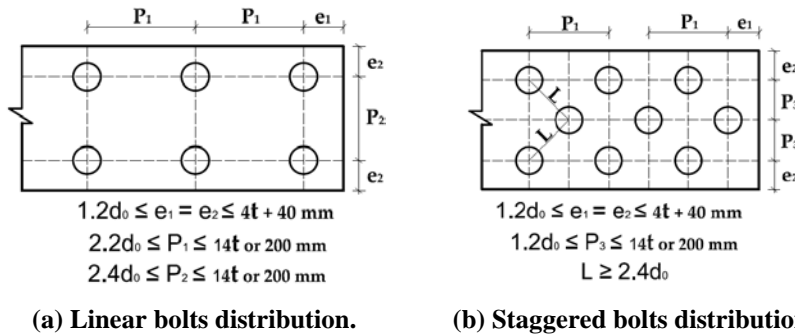

1.2$d_0 \le e_1 = e_2 \le 4t + 40$ mm
2.2$d_0 \le P_1 \le 14t$ or 200 mm
2.4$d_0 \le P_2 \le 14t$ or 200 mm

1.2$d_0 \le e_1 = e_2 \le 4t + 40$ mm
1.2$d_0 \le P_3 \le 14t$ or 200 mm
L $\ge 2.4d_0$

(a) Linear bolts distribution.   **(b) Staggered bolts distribution.**

**Fig. 1. Minimum and maximum spacing symbols for the end "e1",
edge distances "e2", and spacing of bolts connection "P1, P2 and P3" [1].**

The existence of these bolted holes, whether circular or any other shape, in the steel plates, significantly affects the mechanical response of steel structure [3-6]. Because of the specific behaviour of such connections, the numerical study [7-11] as shown in Fig. 2, and in [12-21], the experimental studies have been intensified in this area over the past two decades. Few studies have been conducted to verify the behaviour of steel plate connections with two types of bolts distributed, such as linear bolts distribution and staggered bolts distribution [22, 23], but the literature did not investigate the difference between the distribution of bolts in both linear and staggered distribution. Given the limited number of test results currently available, further examination is necessary to understand the behaviour of these steel structural components to improve existing design provisions and expand the area of their use.
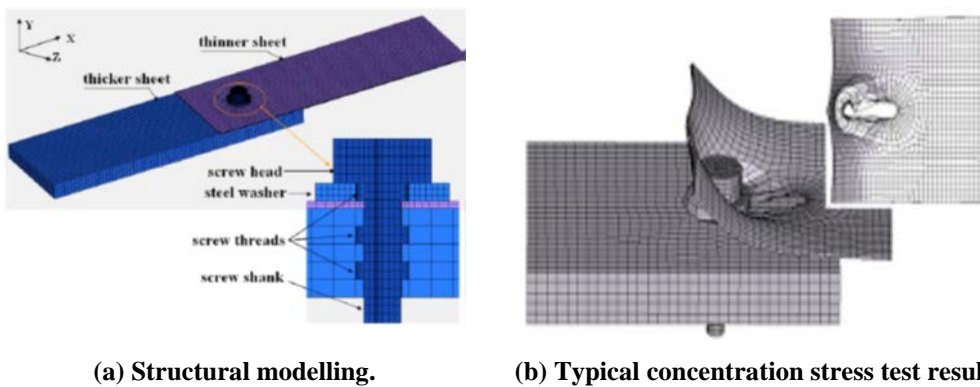

(a) Structural modelling.   **(b) Typical concentration stress test result.**

**Fig. 2. The structural modelling and a typical
concentration stress test result from the numerical study [10].**

In this paper, several parameters were studied, such as the distance between the bolts in the longitudinal and transverse direction, the shape of the bolt distributions such as linear or staggered distribution, and the difference critical net sections of the steel plates. Based on experimental results, improved current design equations for net section stress capacity of steel plate connections are proposed by adding a reduction coefficient for calculated stresses. The steel plates with a thickness of equal to 5 *mm* were studied, which is the thickness that separates between the plates and sheets [24].

2. Net Section Tension Failure Capacity by Current Code Equations

For the tensile rupture of connecting elements, the design rules for steel plate connections covering net section failure in AISC [2] have also been adopted in Eurocode-3 Part 1-1 [25]. Resistance to ultimate tension section fracture stress is given by Eq. (1):

$$\sigma_u = P_u / A_e \qquad (1)$$

where σ_u is the ultimate section fracture tensile stress, P_u is the axial tensile applied ultimate load, and A_e is the effective net section area of steel plate.

If the bolt holes are linear distribution, the total area to be deducted from the area shall be the maximum sum of the areas cut from the holes in any cross-section perpendicular to the axis of the member. Wherefore effective net area as defined in Eq. (2):

$$A_e = A_{total} - t \times (n \times d_o) \qquad (2)$$

where A_{total} is the gross section area of steel plate, t is the thickness of the steel plate, n is the number of holes in one section line, do is the diameter of the bolt hole. Where the bolt holes are staggered, as shown in Fig. 3. The effective net area of tension members should be the least of Eq. (2) for any cross-section, such as section 1 perpendicular to the member axis or Eq. (3) for a chain such as section 2 of holes extending across a part in any diagonal line:

$$A_e = A_{total} - t \times \left(n \times d_o - \sum \frac{S^2}{4g} \right) \qquad (3)$$

Some variables have been rewritten in equations for consistency across different codes. Where the variables S and g are the staggered pitch parallel and perpendicular to the member axis, as shown in Fig. 3.
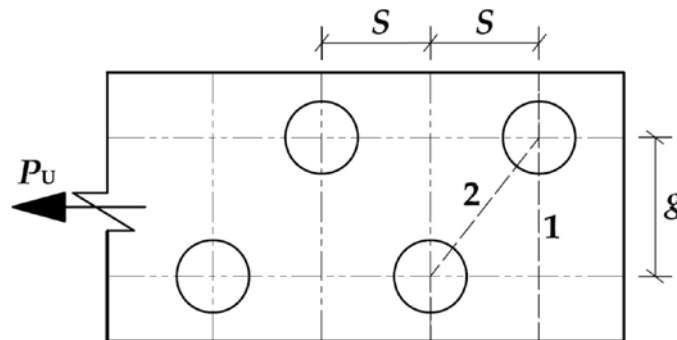

Fig. 3. Staggered bolted holes and critical fracture lines 1 and 2 [25].

All equations in this section apply to connections in steel plates without shear legs and all tension members where the tension load is transferred directly to each element of the cross-section by connection bolts. In the present study, experimental tests have been conducted on single bolted connection, connections with multiple bolts in parallel and perpendicular line of applied load, to verify current design code equations. All samples were configured so that they failed only in the fracture tensile rupture.

3. Experimental Test Specimens

To choose the dimensions of the cross-sections, samples were designed to contain the failure of the type of fracture on the net cross-section, so that the bolts distribution such as linear or staggered connections effect can be evaluated. The experimental testing program examined nine tensile samples of a thickness of 5.0 mm of the same steel grades. Specimens were taken from the same steel plate to ensure that there was no significant change in the mechanical properties of the specimens. The steel plate specimens were divided into three groups. The first group consists of connections with the spacing of bolts equal to 2.4ϕ, where ϕ is the diameter of the bolt hole. The second group consists of connections with the spacing of bolts equal to 3.0ϕ. The third group consists of connections with the spacing of bolts equal to 4.0ϕ. Each group consists of three specimens, a controlled specimen without hole bolts, a specimen with linear distribution connection, and a specimen with staggered distribution, as shown in Fig. 4. Table 1 demonstrates the key geometric characteristics of the test data. The total of nine bolts used to connect the steel plates specimens with 12mm diameter and high strength bolts with grade 8.8. The net critical width is determined by the line passing between the bolt holes in section 1 or section 2, as shown in Fig. 5. The specimens are designed so that each group has the same effective net width so that the difference can be compared and find the effect of different bolts distribution.
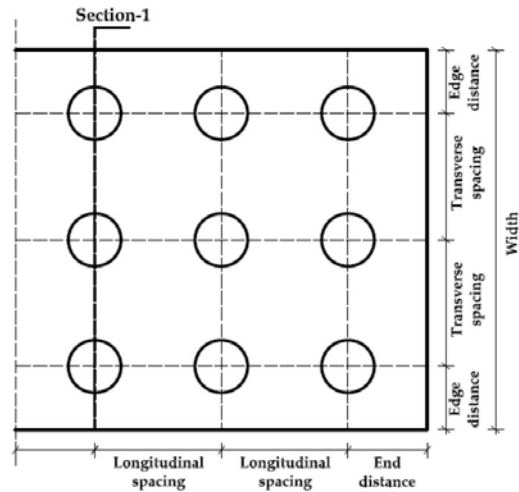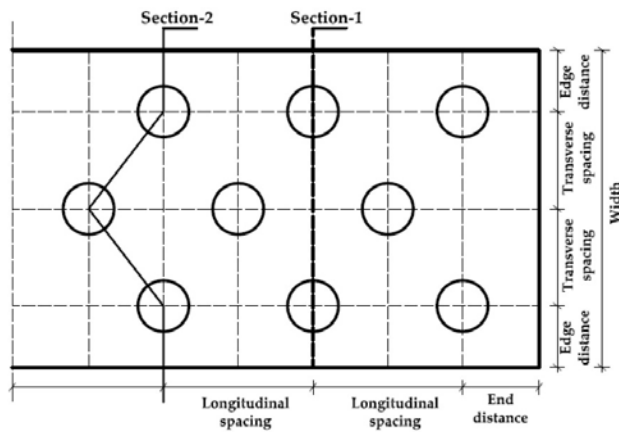

(a) Specimens with 2.4ϕ.   **(b) Specimens with 3.0ϕ.**   **(c) Specimens with 4.0ϕ.**

Fig. 4. Experimental test specimens of the steel plates in the three groups.

(a) Linear bolts distribution.

(b) Staggered bolts distribution.

Fig. 5. Definitions of geometric variables of bolted connections.

Table 1. Description of steel plate connection specimens.

Steel plate specimens	Steel plates characteristics							Bolts offset from centre to centre	
	Width (mm)	Connection type	Net width (mm)		Edge distance (mm)	End distance (mm)		Longitudinal spacing (mm)	Transverse spacing (mm)
			Section-1	Section-2					
C-2.4ϕ	50.4	Control	50.4	-	-	-		-	-
B$_L$-2.4ϕ	86.4	Linear	50.4	-	14.4	18.0		28.8	28.8
B$_S$-2.4ϕ	74.4	Staggered	50.4	50.4	14.4	18.0		35.2	22.8
C-3ϕ	72.0	Control	72.0	-		-		-	-
B$_L$-3ϕ	108.0	Linear	72.0	-	18.0	18.0		36.0	36.0
B$_S$-3ϕ	96.0	Staggered	72.0	72.0	18.0	18.0		40.0	30.0
C-4ϕ	96.0	Control	96.0	-		-		-	-
B$_L$-4ϕ	132.0	Linear	96.0	-	18.0	18.0		48.0	48.0
B$_S$-4ϕ	108.0	Staggered	84.0	96.0	18.0	18.0		64.0	36.0

A 30-ton tensile testing machine was used to conduct all tests. The configuration of the test set is shown in Fig. 6. To ensure that the axially applied loads are in the direction of the centreline of the specimen completely and there is no deviation, causing additional stress is not taken into account was used welded shim plate in all specimens with or without connections, as shown in Fig. 6. A 10 mm thickness gusset plate is used, which is equal to twice the thickness of the steel plate specimen to ensure that the net section fracture will be in the measuring plate.
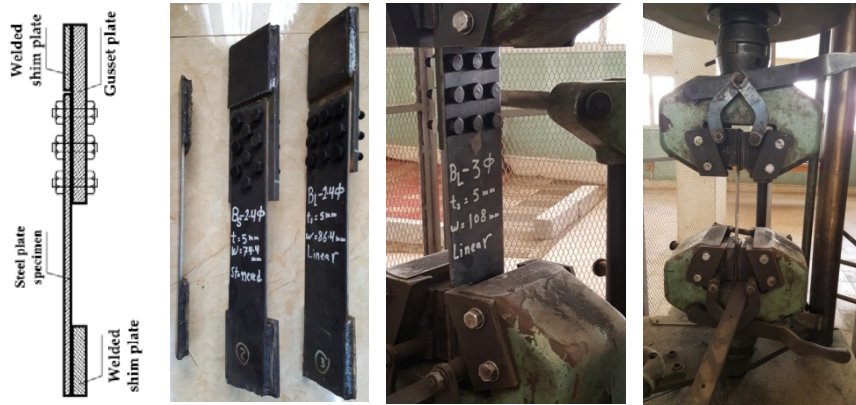

Fig. 6. Arrangements of the test specimens and the clamped ends.

4. Results and Discussions

This study analyses the influence of the axial tension stress state when the steel plate is perforated to connection, as well as the effect of different bolts distribution. In calculating the net section tension stress capacity (σ) of specimens is measured by the values of the load capacity, and the geometric dimensions of the steel plate bolted connections. Table 2 summarizes the details of the experimental investigations into the steel plates behaviour, the failure mode of net section fracture with unfastened, and fastened plates under axial tension load.

**Table 2. Summary of steel plate specimens
based on the experimental results in this study.**

| Steel plate specimens | Connection type | Net fracture | | Yielding load (kN) | Yielding stress | | Ultimate load (kN) | Ultimate stress | |
		width (mm)	Area (mm^2)		σ_y (MPa)	$\sigma_{y.B.}/\sigma_{y.C}$		σu (MPa)	$\sigma u_{.B.}/\sigma u_{.C}$
C-2.4ϕ	Control	50.4	252	62.0	246.03	-	93.5	371.03	-
B$_L$-2.4ϕ	Linear	50.4	252	65.2	258.73	1.052	100.4	398.41	1.074
B$_S$-2.4ϕ	Staggered	50.4	252	55.6	220.63	0.897	76.0	301.59	0.813
C-3ϕ	Control	72.0	360	86.5	240.03	-	130.4	362.22	-
B$_L$-3ϕ	Linear	72.0	360	93.8	260.56	1.086	139.7	388.06	1.071
B$_S$-3ϕ	Staggered	72.0	360	76.9	213.61	0.889	108.1	300.28	0.829
C-4ϕ	Control	96.0	480	120.0	250.00	-	177.0	368.75	-
B$_L$-4ϕ	Linear	96.0	480	127.8	266.25	1.065	186.2	387.92	1.052
B$_S$-4ϕ	Staggered	96.0	480	111.7	232.71	0.931	148.3	308.95	0.838

4.1. Pattern of failure modes.

Failure mode was observed to fracture the net section for all samples connected using linear or staggered distribution bolts connection such as in linear distribution

through the line passing between the bolt holes in section 1, but for the specimens connected using staggered distribution through the line passing between the staggered bolts holes in section 2. A typical failure mode is shown in Fig. 7.

(a) Specimens with 2.4φ.

(b) Specimens with 3.0φ.

(c) Specimens with 4.0φ.

Fig. 7. Failure modes for all specimens in the three groups.

4.2.1. The pattern of maximum ultimate stresses.

From data and experimental analysis, it became clear that the critical section is not the smallest in width but depends on the shape of the line passing through the cross-sections and the force direction that affect it. From specimens BL-4ϕ and BS-4ϕ, as shown in Fig. 8, the location of the failure of net section fracture was observed in section 2 in staggered distribution bolts, which passes through the length equals 96.0*mm*, with inclination angle 48.36⁰ on the direction of the axial force. However, section 1 is the smallest in the width since the length is equal to 84.0*mm* but passes through the linear bolts if it was arithmetically the critical section, the experimental analysis proved otherwise, as shown in Fig. 8(b). This is because section 2 is an inclined angular segment (48.36⁰) on the direction of the axial force, and this gives rise to the existence of strong dual stress in this section. Thus, at the edge of the holes, the stress concentration is always higher than other parts, the crack would initiate at these edges after that, the crack heading to the inclined line between bolts. This dual stress affects the maximum stress that can withstand the critical section. It was found that the stress reduction rate for this section in the yield and maximum ultimate stresses are equal to 6.9% and 16.2%, respectively, of the control specimen. This should, therefore, be taken into consideration during the design process of the steel plate critical section.

| (a) Linear bolts distribution. | (b) Staggered bolts distribution. |

Fig. 8. Net section fracture of specimens with 4.0ϕ.

4.2.1. Yield and maximum ultimate stresses.

In Fig. 9, the effect of the shape of the bolt distribution on the yield and maximum ultimate stresses was observed. It was figured out that the shape of the bolts in a linear distribution affected the increase in the stress capacity of the steel plates, where the average percentage of increase in yielding and maximum stresses were 6.77% and 6.57%, respectively. This increase is considered a safety factor when designing a section that contains a linear distribution of bolts, as no code is specified for this increase. The shape of bolts in the case of staggered distribution has an effect on the decrease in the stress capacity of the steel plates, where the average percentage of decrease in yielding and maximum stresses were 9.43% and 17.33% respectively. This decrease of stress is a very serious risk when designing the steel plate section, where the design codes did not provide for the reduction of stresses when using this shape of the staggered bolts distribution. It is also clear from Fig. 9, that increasing the distance between the bolts, the less their impact on the stresses.

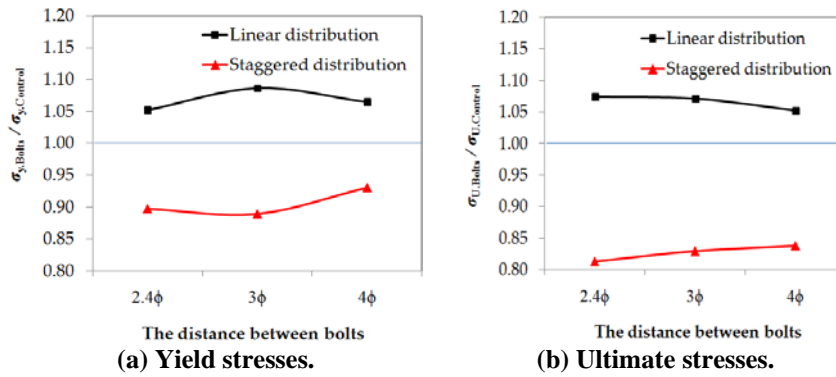(a) Yield stresses.   (b) Ultimate stresses.

Fig. 9. Relation between the ratio of net section steel plate bolted connection to control solid steel plate stresses and the influence of the bolt distribution shapes.

5. Comparison of the Experimental Results of the Specimen BS-4ϕ with the Numerical Simulation.

The specimen BS-4ϕ was selected because the expected results and the location of the fracture were different from the site of the current design code. In order to increase the assurance of experimental results and it is not just a coincidence, numerical analysis by three-dimensional finite element modelling was used where it proved that it has high accuracy in the modelling of steel structures [6-11].

SOLID186 element ANSYS-15 [26] program was employed for modelling the steel plate with a solid element. The SOLID186 was definition as 20 nodes having 3-degrees of freedom at each node, as shown in Fig. 10. This element allows specific properties from the other models [26] in addition to the capability to simulate the deformations of elastic-plastic materials. Based on the results of an experimental test of specimen C-4ϕ which is the control for the specimen BS-4ϕ, the engineering stress-strain relationship of the tension test results is applied to FE modelling, as shown in Table 3, with elastic modulus concerning $210 GPa$ and a Poisson ratio of 0.3.
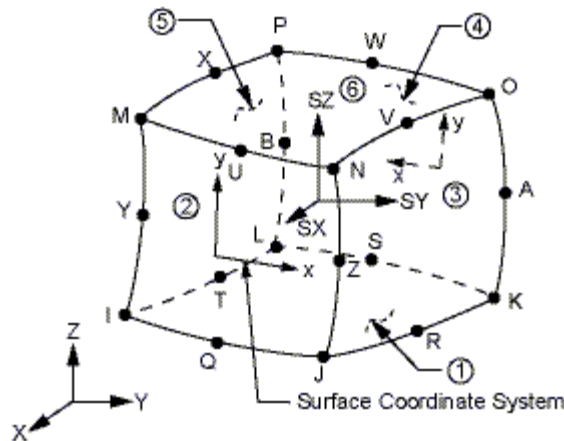

Fig. 10. SOLID186 homogeneous structural solid geometry [26].

Table 3. Engineering stress-strain relationship of the FE simulation.

Stress (MPa)	250	292	301	324	342	360	368	353
Corresponding Strain	0.00119	0.0039	0.0101	0.0326	0.0549	0.091	0.1253	0.1804

From the process of numerical analysis, it turned out that the place of net section fracture is also section 2 and that the concentration of stresses on this section, as shown in Fig. 11. It is quite applicable to experimental testing, as mentioned before, in Fig. 8(b). The yielding and maximum loads capacity for this specimen BS-4ϕ were equal to 113.29 kN and 150.47 kN, respectively, so the yielding and maximum stresses in section 2 are equal to 236.02 MPa and 313.48 MPa, respectively. Thus, the ratios between the yielding and ultimate stresses from numerical analysis to experimental test 1.014 and 1.015, respectively, which this means the numerical analysis is very close to the experimental measurements for the same specimen.
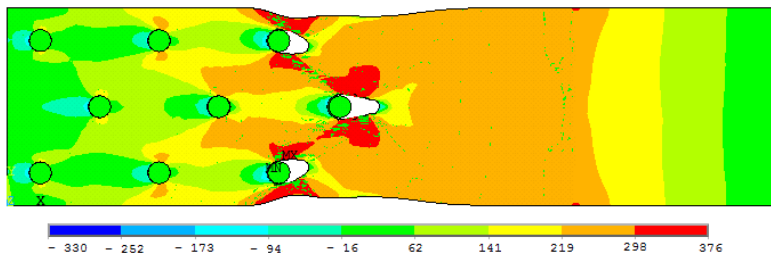

Fig. 11. The stress concentration from the numerical simulation of the specimen BS-4ϕ with the staggered distribution.

In order to ensure more use of numerical analysis compared to experimental tests, the numerical analysis was done on the sample BL-4ϕ with linear bolts distribution. From the process of numerical analysis, it turned out that the place of net section fracture is section 1 and that the concentration of stresses on this section, as shown in Fig. 12. It is quite applicable to experimental testing, as mentioned before, in Fig. 8(a). The yielding and maximum loads capacity for this specimen BL-4ϕ were equal to 130.48 kN and 184.60 kN, respectively, so the yielding and maximum stresses in section 1 are equal to 271.83 MPa and 384.58 MPa, respectively. Thus, the ratios between the yielding and ultimate stresses from numerical analysis to experimental test 1.021 and 0.991, respectively.
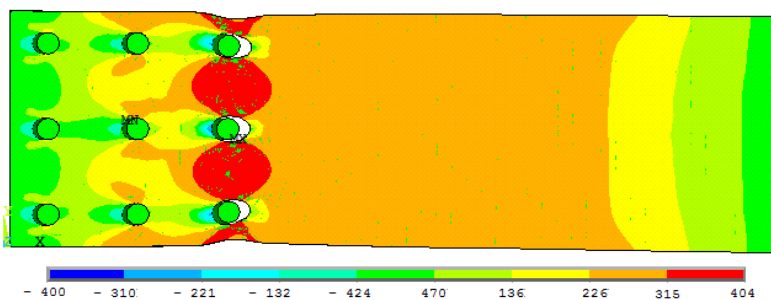

Fig. 12. The stress concentration from the numerical simulation of the specimen BL-4ϕ with a linear distribution.

6. Comparison of the Experimental Results with the Design Codes.

To evaluate the reliability of the predicted results obtained from the current design codes proposed by AISC [2], and Eurocode-3 [25], we used the current design Eqs. (2) and (3) to compare them with the results obtained from the experimental results. Table 4 shows the ultimate failure stress for both current design codes [2, 25] and experimental results with the ratios between them. The experimental and analytical values are compared graphically in Fig. 13. In this table and figure, for the ultimate stress capacities of linear bolts distribution, the mean value calculated form current design codes of σu. Code./σu.C. is 1.00; this means that the expected values can be used in design processes where it is less than the average actual values σu.Exp./σu.C = 1.065. Nevertheless, for the staggered bolts distribution, the mean value calculated form current design codes of σu.Code./σu.C. is 1.112; this means that the expected values cannot be used in design processes where it is more than the average actual values σu.Exp./σu.C = 0.827. These values illustrate that the current design codes [2, 25] is an exceptional match and can be adopted for linear bolts distribution but does not agree with staggered bolts distribution.

Table 4. A comparison between the ultimate failure stresses obtained from an experimental test with the current design codes.

| Steel plate specimens	Connection type	Experimental			AISC and Eurocode-3 codes Eq. (1)		
		Ultimate load (kN)	$\sigma u_{.Exp.}$ (MPa)	$\sigma u_{.Exp.}/\sigma u_{.C}$	Effective net width (mm)	$\sigma u_{.Code}$ (MPa)	$\sigma u_{.Code}/\sigma u_{.C}$
C-2.4ϕ	Control	93.5	371.03	-	50.4	371.03	1.000
B$_L$-2.4ϕ	Linear	100.4	398.41	1.074	50.4	371.03	1.000
B$_S$-2.4ϕ	Staggered	76.0	301.59	0.813	45.2	413.72	1.115
C-3ϕ	Control	130.4	362.22	-	72.0	362.22	1.000
B$_L$-3ϕ	Linear	139.7	388.06	1.071	72.0	362.22	1.000
B$_S$-3ϕ	Staggered	108.1	300.28	0.829	66.7	391.00	1.079
C-4ϕ	Control	177.0	368.75	-	96.0	368.75	1.000
B$_L$-4ϕ	Linear	186.2	387.92	1.052	96.0	368.75	1.000
B$_S$-4ϕ	Staggered	148.3	308.95	0.838	84.0	421.43	1.143
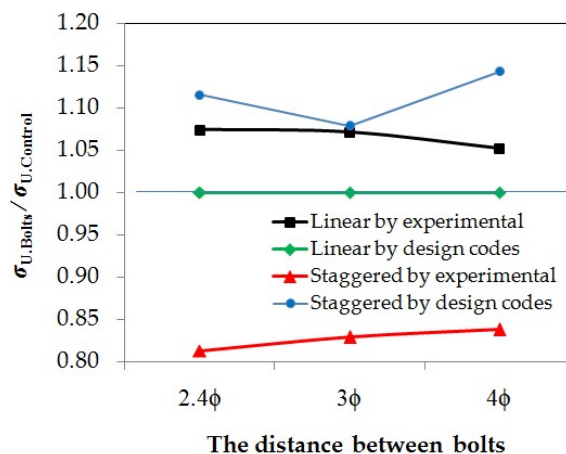
Fig. 13. A comparison between the experimental and the current design codes for the ultimate-failure stress capacity.

In Fig. 14 there is a 45-degree inclined line that divides the shape into two sides [22], one side is safe side in that the calculated stress is less than the actual stress and the other side it is unsafe where the calculated values of stress are greater than the actual stress. It can be seen that the results come from current design codes [2, 25] for linear bolts distribution fall within the safe side, but for staggered bolts distribution, the results come from current design codes [2, 25] fall within the unsafe side. This shows that in the current design codes [2, 25], there is a problem to predict the values of stress in the staggered bolts distribution, and they need to modify.
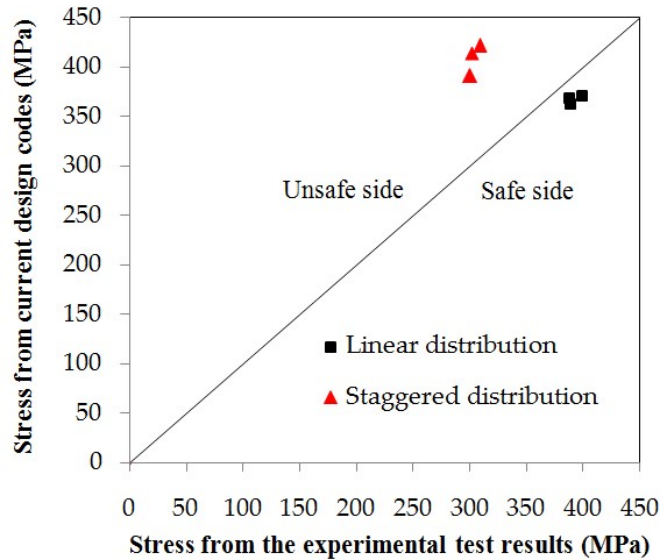

Fig. 14. Predicted ultimate-failure stress capacity by the current design codes in comparison with the experimental values.

7. Conclusions.

The validated experimental test has been used to investigate the fracture of the net section and ultimate-failure stress capacity of steel plate connections under static axial tension load. Parametric studies were conducted to assess the effects of bolt distribution types, and the spacing between bolts on the capacity of the yield and maximum ultimate stresses, of the steel plate connections. The parametric studies showed the following:

- The critical net section area is not always the smallest width. However, it depends on the shape of the bolt distribution, such as the staggered distribution is often the critical section even if it is the longest in terms of net width.

- The shape of the bolts in a linear distribution affected the increase in the stress capacity of the steel plates, where the average percentage of increase in yielding and maximum stresses were 6.77% and 6.57%, respectively. This increase is considered a safety factor when designing a section as no current design codes are specified for this increase.

- In staggered bolts distribution, the stress reduction rate in the yielding and maximum ultimate stresses are equal to 9.43% and 17.33%, respectively.

- The current design codes [2, 25] calculations of the ultimate stress capacities of linear bolts distribution are applicable and have some factor of safety. Nevertheless, on the other side, the codes calculations of the ultimate stress capacities of staggered bolts distribution are unsuitable for our case study and need a reduction coefficient at least equal to 0.744 just to get the actual stress of steel plate.

Acknowledgments.

Nomenclatures	
A_e	Effective net section area of steel plate, mm^2
A_{total}	Gross section area of steel plate, mm^2
d_o	The diameter of the bolt hole, mm
g	Staggered pitch perpendicular to the member axis, mm
n	Number of holes in one section line
P_u	Axial tensile applied ultimate load, kN
S	Staggered pitch parallel to the member axis, mm
t	The thickness of the steel plate, mm
Greek Symbols	
σu	Ultimate section fracture tensile stress, MPa
$\sigma u_{.c}$	Ultimate section fracture tensile stress for control specimen, MPa
$\sigma u_{.Code}$	Ultimate section fracture tensile stress from design codes, MPa
$\sigma u_{.Exp}$	Ultimate section fracture tensile stress from experimental test, MPa
σ_y	Yielding tensile stress, MPa
$\sigma_{y.c}$	Yielding tensile stress for control specimen, MPa
ϕ	The diameter of the bolt hole, mm^2

References.

1. BS EN 1993-1-8. (2005). Eurocode 3: *Design of steel structures part 1-8: Design of joints*, British Standard Institute, London.

2. ANSI/AISC 360-16 (2016). *Specification for structural steel buildings*, American Institute of Steel Construction, Chicago.

3. Lee, Y.C.; and Chen, F.K. (2000). Yield criterion for a perforated sheet with a uniform triangular pattern of round holes and a low ligament ratio. *Journal of Materials Processing Technology,* 103(3), 353-361.

4. Maiorana, E.; Pellegrino, C.; and Modena, C. (2008). Linear buckling analysis of perforated plates subjected to localised symmetrical load. *Engineering Structures*, 30(11), 3151-3158.

5. Saraçoğlu, M.H.; and Albayrak, U. (2015). Linear static analysis of perforated plates with round and staggered holes under their self-weights. *Research on Engineering Structures and Materials*, 2, 39-47.

6. Sayed, A.M. (2019). Numerical analysis of the perforated steel sheets under uni-axial tensile force. *Metals*, 9(6), 632.

7. Fan, L.; Rondal, J.; and Cescotto, S. (1997). Finite element modelling of single lap screw connections in steel sheeting under static shear. *Thin-Walled Structures*, 27(2), 165-185.

8. Chung, K.F.; and Ip, K.H. (2000). Finite element modelling of bolted connections between cold-formed steel strips and hot rolled steel plates under static shear loading. *Engineering Structures*, 22(10), 1271-1284.

9. Ju, S.H.; Fan, C.Y.; and Wu, G.H. (2004). Three-dimensional finite elements of steel bolted connections. *Engineering Structures*, 26(3), 403-413.

10. Lu, W.; Mäkeläinen, P.; and Outinen, J. (2008). Finite element modelling of single lap shear screw connection in steel sheeting in fire. *The Open Construction and Building Technology Journal*, 2(1), 257-261.

11. Kim, T.S.; Kuwamura, H.; and Cho, T.J. (2008). A parametric study on ultimate strength of single shear bolted connections with curling. *Thin-Walled Structures*, 46(1), 38-53.

12. Rogers, C.A.; and Hancock, G.J. (1999). Bolted connection design for sheet steels less than 1.0 *mm* thick. *Journal of Constructional Steel Research*, 51(2), 123-146.

13. Puthli, R.; and Flischer, O. (2001). Investigation on bolted connections for high strength steel members. *Journal of Constructional Steel Research*, 57(3), 313-326.

14. Lim, J.B.P.; and Nethercot, D.A. (2004). Stiffness prediction for bolted moment-connections between cold-formed steel members. *Journal of Constructional Steel Research*, 60(1), 85-107.

15. Buđevac, D.; Dobrić, J.; Fric, N.; Knežević, M.; and Marković, Z. (2012). Specific behaviour of thin-walled member joints with fasteners. *Građevinar*, 64(3), 217-230.

16. Teh, L.H.; and Gilbert, B.P. (2012). Net section tension capacity of bolted connections in cold-reduced steel sheets. *Journal of Structural Engineering*, 138(3), 337-344.

17. Wang, Y.B.; Lyu, Y.F.; and Li, G.Q. (2018). Experimental investigation of two-bolt connections for high strength steel members. *12th International Conference on Advances in Steel-Concrete Composite Structures* (ASCCS 2018), Universitat Politècnica de València, València, Spain, June 27-29.

18. Kim, T.; Kim, M.; and Cho, T. (2018). Parametric study on ultimate strength of four-bolted connections with cold-formed carbon steel. *International Journal of Steel Structures*, 18(1), 265-280.

19. Jang, S.; Nam, J.; Lee, S.; and Oh, J.H. (2019). A simple, reusable and low-cost LVDT-based in situ bolt preload monitoring system during fastening for a truck wheel assembly. *Metals*, 9(3), 336.

20. Le, V.T.; Goo, N.S.; and Kim, J.Y. (2019). Thermomechanical behaviour of superalloy thermal protection system under aerodynamic heating. *Journal of Spacecraft and Rockets*, 56(5), 1432-1448.

21. Le, V.T.; Ha, N.S.; Goo, N.S.; and Kim, J.K. (2019). Insulation system using high-temperature fibrous insulation materials. *Heat Transfer Engineering*, 40(17-18), 1523-1538.

22. Salih, E.L.; Gardner, L.; and Nethercot, D.A. (2010). Numerical investigation of net section failure in stainless steel bolted connections. *Journal of Constructional Steel Research*, 66(12), 1455-1466.

23. Nethercot, D.A.; Salih, E.L.; and Gardner, L. (2011). Behaviour and design of stainless-steel bolted connections. *Advances in Structural Engineering*, 14(4), 647-658.

24. ASTM A370/ASME SA-370: (2016). *Standard test methods and definitions for mechanical testing of steel products.* American Society for Testing and Materials, PA, USA.

25. BS EN 1993-1-1: 2005 Eurocode 3: (2005). *Design of steel structures part 1-1: general rules and rules for building*, British Standards Institution, London.

26. ANSYS User's Manual; Version -15 (2015). *Swanson analysis systems. Inc.:* Cannonsburg, PA, USA.